Int. J. Heat Mass Transfer. Vol. 17, pp. 1337–1348. Pergamon Press 1974. Printed in Great Britain

MIXED CONVECTION IN AN ISOTHERMALLY HEATED HORIZONTAL PIPE

C. A. HIEBER* and S. K. SREENIVASAN

Mechanical Engineering Department, Clarkson College of Technology, Potsdam, New York 13676, U.S.A.

(*Received* 2 *July* 1973 *and in revised form* 5 *February* 1974)

Abstract—A theoretical investigation is made into the laminar flow of a large-Prandtl-number fluid through an isothermally heated horizontal pipe. A detailed analytical solution is obtained which shows, in leading approximation, that the fractional bulk-temperature rise is solely a function of $(L/aR)(G/P^3)^{1/4}$. The theory is found to agree very well with available experimental results and to be a marked improvement over existing empirical correlations.

NOMENCLATURE

a, pipe radius;
g, gravitational acceleration (directed along $\varphi = 0$);
G, pipe Grashof number, $\equiv g\beta\Delta T a^3/\nu^2$;
L, pipe length;
N, local Nusselt number, $\equiv q_w a/(k\Delta T)$;
$\bar{N}$, Nusselt number averaged over ϕ;
$\bar{\bar{N}}$, Nusselt number averaged over ϕ and z;
p, pressure;
P, Prandtl number;
q_w, local heat flux, $= k(\partial T/\partial r)_{r=a}$;
r, radial coordinate;
R, pipe Reynolds number, $\equiv aW_0/\nu$;
T_a, average of bulk temperatures at inlet and outlet;
T_b, bulk (or "mixing cup") temperature;
T_0, uniform temperature at inlet;
T_w, wall temperature (uniform);
u, radial velocity component;
v, ϕ-component velocity;
V_B, $\equiv (\nu/a)(G/P)^{1/2}$;
$\tilde{V}_B$, $\equiv \frac{\nu}{a}\left(\frac{z}{aR}\right)\frac{G}{P^{2/3}}$;
w, axial velocity component;
W_0, uniform inlet velocity (or bulk velocity);
z, axial coordinate.

Greek symbols

α, $\equiv 0{\cdot}33206$;
β, coefficient of thermal expansion;
δ, $\equiv \sqrt{(\lambda z)}$;
δ_{th}, $\equiv \delta/P^{1/3}$;
δ_B, $\equiv a/(GP)^{1/4}$;
ΔT, $\equiv T_w - T_0$;
ΔT_b, bulk-temperature rise;
ε_1, $\equiv (z/aR)^2(G/P^{1/3})$;
ε_2, $\equiv (aR/z)^{3/2}(P/G^3)^{1/4}$;
ε_3, $\equiv (z/aR)(G/P^3)^{1/4}$;
ζ, $\equiv (a-r)/\delta_B$;
η, $\equiv \zeta \sin^{1/3}\phi/\xi^{1/4}$;
κ, $\equiv \chi P^{1/3}$;
λ, $\equiv \nu/W_0$ ("viscous length");
μ, dynamic viscosity;
ν, kinematic viscosity;
ξ, $\equiv \int_0^{\phi} \sin^{1/3} t\,dt$;
ρ, fluid density;
ϕ, angular (azimuthal) coordinate;
Φ, $\equiv (\mu_w/\mu_a)^{0{\cdot}14}(\Delta T_b/\Delta T)_{\exp}$;
χ, $\equiv (a-r)/\delta$;
ψ, streamfunction.

Subscripts

a, evaluated at T_a;
B, buoyancy-induced;
exp, experimental;
F, forced-flow-induced;
w, value at wall.

1. INTRODUCTION

THE PRESENT paper is a theoretical investigation of the velocity and temperature development in an isothermally heated horizontal pipe. The analysis corresponds to the large-Prandtl-number limit of the laminar, mixed-convection regime.

Theoretical investigation of this problem has been systematically avoided in the literature due to the

*Presently, Upson Hall, Cornell University, Ithaca, New York 14850, U.S.A.

attendant complexities arising from the three-dimensionality of the flow situation. Instead, all previous analyses of the horizontal orientation have been confined to the fully-developed region of the uniform-heat-flux pipe. Notable examples are the perturbation–expansion solutions of Morton [1], del Casal and Gill [2], Mikesell [3] and Faris and Viskanta [4], the boundary-layer analyses of Mikesell [3], Mori and Futagami [5] and Siegwarth *et al.* [6], and the numerical solutions of Siegwarth and Hanratty [7] and Newell and Bergles [8]. Briefly, the perturbation–expansion results apply to the flow regime in which G is sufficiently small such that the natural convection is a small perturbation upon the forced-flow situation; at the other extreme, the boundary-layer analyses apply to the regime in which G is sufficiently large such that the structure of the flow is buoyancy-dominated and characterized by a thermal boundary layer, of order $a/(GP)^{1/4}$ in thickness, which surrounds a core region. In all instances, the axial dependence of the flow variables is degenerate, consisting solely of a linear drop in the pressure and a linear rise in the bulk temperature.

As is shown in the present investigation, the development of the velocity and temperature fields within an isothermal horizontal pipe consists of a succession of regions, proceeding in the axial direction: a "near region", where buoyancy is a small perturbation upon the forced flow; an "intermediate region", where natural convection is dominant and the thermal boundary layer is axially invariant, its thickness being of order $a/(GP)^{1/4}$, as above; a "break-up region", where the core region interacts with the thermal boundary layer as the bulk-temperature rise in the core becomes of order ΔT and the natural-convection effect therefore diminishes; a "far-region", where the forced convection reappears as the dominant transport mechanism and the fluid temperature approaches T_w asymptotically in a Graetz-like manner. Although the near- and intermediate regions can be expected to exhibit similarities to the above-mentioned perturbation- and boundary-layer analyses, respectively, a significant difference is that now, for given inlet conditions, a whole gamut of flow regimes exist simultaneously along the pipe. (Of course, such a situation also obtains in the uniform-heat-flux case for which, however, the previous analyses have been concerned only with the final, fully-developed region which, as noted above, "degenerates" into the Graetz problem in the isothermal-pipe case.) For practical purposes, it is the breakup region which is of primary interest since it is here that the bulk-temperature rise becomes appreciable and, hence, where comparison with existing experimental data can be made.

Experimentally, the isothermal horizontal pipe has been investigated for various large-Prandtl-number fluids. Notable examples are the studies by Kern and Othmer [9] in three different oils, Oliver [10] in water, ethyl alcohol, 80:20 glycerol–water and glycerol, Brown and Thomas [11] in water, and Depew and August [12] in water, ethyl alcohol and 80:20 glycerol–water. Comparison of these experimental results with the present theory is given in Section 3, where the fractional rise in bulk temperature is plotted vs $(L/aR)(G/P^3)^{1/4}$, this latter quantity arising naturally from the theory as being the controlling parameter for large-P fluids. Agreement between the zeroth-order theory (as $P \to \infty$) and the experimental data in water, ethyl alcohol and 80:20 glycerol–water is found to be good, the average deviation being approximately 6, 12 and 15 per cent, respectively. By accounting for higher-order effects, the agreement is brought to within about 3, 8 and 10 per cent, respectively. The glycerol data, which is largely forced-flow dominated (as intended by Oliver) is still brought to within an average deviation of $\approx$ 20 per cent after higher-order "corrections" (rather large in this case) are made. Lastly, the data of Kern and Othmer show a systematic dependence upon the pipe radius which is not explainable in terms of the present theory but which is conjectured as being due to thermal instabilities in the larger-sized pipes. In particular, the data in the largest-radius pipe shows an average deviation of about 45 per cent below the theory whereas, in the smallest pipe, the average deviation is $\lesssim$ 10 per cent for two of the three oils.

A detailed analysis of the problem under consideration is given in Section 2. This is followed in Section 3 by a discussion which includes a detailed comparison with the above experimental investigations.

2. ANALYSIS

The physical situation being investigated is one in which a large-Prandtl-number fluid flows through an isothermally heated, horizontal pipe of radius a and temperature T_w. At pipe inlet, the fluid has a uniform axial velocity profile, $w = W_0$, and temperature, $T = T_0$. The flow is assumed to remain laminar, thereby requiring that the pipe Reynolds number, $R \equiv W_0 a/\nu$, be $\lesssim 10^3$. On the other hand, the analysis assumes that the unperturbed flow (i.e. with buoyancy omitted) exhibits a boundary-layer structure during part of its development, thereby requiring $R \gtrsim 10^2$. (The major result of the present investigation is not actually subject to this latter constraint, as will become clear later.) The usual Boussinesq approximation will be employed in handling buoyancy effects and viscous dissipation will be neglected.

(a) *The near region*

If natural convection is neglected, it is well-known that the velocity field is characterized by a boundary

layer surrounding an inviscid core in the region

$$O\left(\frac{1}{R^2}\right) < \frac{z}{aR} < O(1). \tag{2.1}$$

In leading approximation, the velocity boundary layer is described by Blasius flow over a flat plate:

$$\psi_F = W_0 \delta F(\chi), \quad w_F = -\frac{\partial \psi_F}{\partial r}, \quad u_F = \frac{\partial \psi_F}{\partial z} \tag{2.2}$$

where $F''(0) = 0{\cdot}33206 \equiv \alpha$. The well-known temperature distribution associated with the above flow is given by:

$$T_F = T_0 + \Delta T\, H(\kappa), \quad H(\kappa) = A \int_\kappa^\infty e^{-\alpha t^{3/2}} dt \tag{2.3}$$

where

$$A = (9\alpha/4)^{1/3}/\Gamma(\tfrac{1}{3}) = 0{\cdot}33872.$$

Basing the buoyant force upon (2.3), in leading approximation, it follows that the limiting equations of motion for the buoyancy-induced field in the thermal boundary layer are:

$$\frac{\partial v_B}{a\,\partial \phi} + \frac{\partial u_B}{\partial r} = 0 \tag{2.4}$$

$$\nu \frac{\partial^2 v_B}{\partial r^2} + g\beta \Delta T H \sin\phi = 0 \tag{2.5}$$

with the radial force balance being hydrostatic (see [13]). Hence, this leading buoyancy-induced motion can be represented by

$$\left.\begin{aligned} \psi_{B1} &= \tilde{V}_B \delta_{th} F_1(\kappa) \sin\phi \\ v_{B1} &= -\frac{\partial \psi_{B1}}{\partial r} = \tilde{V}_B F_1'(\kappa) \sin\phi, \\ u_{B1} &= \frac{\partial \psi_{B1}}{a\,\partial \phi} = \frac{\delta_{th}}{a} \tilde{V}_B F_1 \cos\phi \end{aligned}\right\} \tag{2.6}$$

where F_1 is governed by

$$F_1''' = -H \qquad F_1(0) = 0 = F_1'(0) = F_1''(\infty). \tag{2.7}$$

Numerical integration results in:

$$F_1''(0) = 1{\cdot}67115, \quad F_1'(\infty) = 2{\cdot}04010. \tag{2.8}$$

In turn, u_{B1} convects T_F, thereby giving rise to T_{B1} which can be represented by

$$T_{B1} = \varepsilon_1 \Delta T H_1(\kappa) \cos\phi \tag{2.9}$$

and is governed by

$$\left.\begin{aligned} H_1'' + \frac{\alpha}{4}\kappa^2 H_1' - 2\alpha\kappa H_1 &= -F_1 H', \\ H_1(0) = 0 &= H_1(\infty) \end{aligned}\right\} \tag{2.10}$$

which, upon numerical integration, results in

$$H_1'(0) = -0{\cdot}21770. \tag{2.11}$$

Second-order terms in the buoyancy-induced motion evidently arise from T_{B1}. In turn, the resulting thermal convection of T_F by u_{B2}, and that of T_{B1} by v_{B1} and u_{B1}, induces T_{B2}. In particular,

$$\left.\begin{aligned} \psi_{B2} &= \varepsilon_1 \tilde{V}_B \delta_{th} F_2(\kappa) \sin\phi \cos\phi \\ T_{B2} &= \varepsilon_1^2 \Delta T [H_{21}(\kappa) + \sin^2\phi H_{22}(\kappa)] \end{aligned}\right\} \tag{2.12}$$

and numerical integration of the governing equations for F_2, H_{21} and H_{22} (see [13]) results in:

$$\left.\begin{aligned} F_2''(0) &= -0{\cdot}90642, \quad F_2'(\infty) = -2{\cdot}08348 \\ H_{21}'(0) &= \;\; 0{\cdot}05575, \quad H_{22}'(0) = -0{\cdot}28494 \end{aligned}\right\} \tag{2.13}$$

In particular, then, the leading terms in the buoyancy-induced heat transfer are given by

$$\begin{aligned} k\left(\frac{\partial T_B}{\partial r}\right)_{r=a} &= \frac{k\Delta T}{\delta_{th}} \{0{\cdot}2177\varepsilon_1 \cos\phi + \varepsilon_1^2 \\ &\quad \times [-0{\cdot}0558 + 0{\cdot}2849 \sin^2\phi] + O(\varepsilon_1^3)\}. \end{aligned} \tag{2.14}$$

Hence, integrated over ϕ, the leading contribution is $0{\cdot}0867\varepsilon_1^2 k\Delta T/\delta_{th}$.

In order that the above be self-consistent, it is clearly required that $\varepsilon_1 < O(1)$, i.e. $z/aR < O(P^{1/6}/G^{1/2})$. Hence, if $G > O(P^{1/3})$ it follows that natural convection becomes significant where $z/aR < O(1)$ and the above expansion is restricted to the region

$$O\left(\frac{1}{R^2}\right) < \frac{z}{aR} < O\left(\frac{P^{1/6}}{G^{1/2}}\right). \tag{2.15}$$

On the other hand, if $G < O(P^{1/3})$ then the axial flow becomes fully developed at $z/aR = O(1)$ with buoyancy still being negligible. The subsequent development of the thermal boundary layer is then within Poiseuille flow—the Leveque problem, in leading approximation—with the natural convection becoming significant where $z/aR = O(P^{1/4}/G^{3/4})$. In particular, then, since the forced-flow-dominated temperature field is known to become fully developed (i.e. $T_F \sim T_W$) where $z/aR = O(P)$, it follows that natural convection never becomes important if $G < O(P^{-1})$.

(b) *The intermediate region*

The results in (a) imply that if $G > O(P^{1/3})$ then the thermal boundary layer is buoyancy-dominated once $z/aR > O(P^{1/6}/G^{1/2})$. Hence, proceeding in a manner similar to that above but now with the forced flow assumed negligible, the limiting ϕ-momentum and energy equations in the thermal boundary layer become:

$$0 = \nu \frac{\partial^2 v_B}{\partial r^2} + g\beta(T_B - T_0)\sin\phi \tag{2.16}$$

$$\left(v_B \frac{\partial}{a\,\partial\phi} + u_B \frac{\partial}{\partial r}\right) T_B = \frac{\nu}{P} \frac{\partial^2 T_B}{\partial r^2} \tag{2.17}$$

with u_B again being coupled to v_B via the continuity equation, (2.4), and the radial force balance again being hydrostatic. Appropriate expansions for these buoyancy-dominated quantities are therefore given by

$$\left.\begin{aligned} &\psi_B = V_B \delta_B \hat{f}(\zeta,\phi), \qquad T_B = T_0 + \Delta T \hat{h}(\zeta,\phi) \\ &v_B = -\frac{\partial \psi_B}{\partial r} = V_B \frac{\partial \hat{f}}{\partial \zeta}, \quad u_B = \frac{\partial \psi_B}{a\,\partial \phi} = \frac{\delta_B}{a} V_B \frac{\partial \hat{f}}{\partial \phi} \end{aligned}\right\} \tag{2.18}$$

with the non-dimensionalized governing equations becoming

$$\frac{\partial^3 \hat{f}}{\partial \zeta^3} + \hat{h} \sin\phi = 0 \tag{2.19}$$

$$\frac{\partial^2 \hat{h}}{\partial \zeta^2} + \frac{\partial \hat{f}}{\partial \phi}\frac{\partial \hat{h}}{\partial \zeta} - \frac{\partial \hat{f}}{\partial \zeta}\frac{\partial \hat{h}}{\partial \phi} = 0 \tag{2.20}$$

subject to the conditions:

$$\begin{aligned} &\hat{f}(0,\phi) = 0 = \frac{\partial \hat{f}}{\partial \zeta}(0,\phi), \quad \hat{h}(0,\phi) = 1; \\ &\frac{\partial^2 \hat{f}}{\partial \zeta^2}(\infty,\phi) = 0 = \hat{h}(\infty,\phi). \end{aligned} \tag{2.21}$$

As was shown by Acrivos [14] for an analogous problem, (2.19)–(2.21) can be reduced to similarity form (a consequence of $P \to \infty$ and the attendant neglect of the inertial effect). An appropriate transformation is given by

$$\left.\begin{aligned} &\xi \equiv \int_0^\phi \sin^{1/3} t \, dt, \qquad \eta \equiv \frac{\sin^{1/3}\phi}{\xi^{1/4}} \zeta \\ &\hat{f}(\zeta,\phi) = \xi^{3/4} f(\eta), \qquad \hat{h}(\zeta,\phi) = h(\eta) \end{aligned}\right\} \tag{2.22}$$

which results in

$$\left.\begin{aligned} &f''' + h = 0, \quad h'' + \tfrac{3}{4} f h' = 0; \quad f(0) = 0 = f'(0), \\ &h(0) = 1, \quad f''(\infty) = 0 = h(\infty). \end{aligned}\right\} \tag{2.23}$$

The solution of (2.23) has the following well-known properties:

$$\left.\begin{aligned} &f''(0) = 1{\cdot}16604, \quad h'(0) = -0{\cdot}50275 \\ &f(\eta) \sim 1{\cdot}02136\eta - 0{\cdot}73825 \quad \text{as} \quad \eta \to \infty. \end{aligned}\right\} \tag{2.24}$$

In particular, the ϕ-averaged heat flux is given by

$$\begin{aligned} \frac{1}{\pi}\int_0^\pi k\left(\frac{\partial T}{\partial r}\right)_{r=a} d\phi &= -k\frac{\Delta T}{\delta_B}\frac{h'(0)}{\pi}\int_0^\pi \frac{\sin^{1/3}\phi \, d\phi}{\xi^{1/4}} \\ &= 0{\cdot}43526 \frac{k\Delta T}{a}(GP)^{1/4}. \end{aligned} \tag{2.25}$$

(c) *The near-intermediate region*

The perturbation effect of the forced flow upon the structure of (b) arises from $u_F(\partial T_B/\partial r)$ with the limiting ϕ-momentum and energy equations being

$$0 = \nu \frac{\partial^2 v_{F1}}{\partial r^2} + g\beta T_{F1} \sin\phi \tag{2.26}$$

$$\left(v_B \frac{\partial}{a\,\partial\phi} + u_B \frac{\partial}{\partial r}\right) T_{F1} + \left(v_{F1}\frac{\partial}{a\,\partial\phi} + u_{F1}\frac{\partial}{\partial r} + u_F \frac{\partial}{\partial r}\right) T_B = \frac{\nu}{P}\frac{\partial^2 T_{F1}}{\partial r^2}. \tag{2.27}$$

If u_F is based upon Blasius flow, (2.2), then an appropriate representation of these first-order perturbation quantities is given by

$$\left.\begin{aligned} &\psi_{F1} = \varepsilon_2 V_B \delta_B \hat{\mathscr{F}}_1(\zeta,\phi), \quad T_{F1} = \varepsilon_2 \Delta T \hat{\mathscr{H}}_1(\zeta,\phi) \\ &v_{F1} = \varepsilon_2 V_B \frac{\partial \hat{\mathscr{F}}_1}{\partial \zeta}, \qquad u_{F1} = \varepsilon_2 V_B \frac{\delta_B}{a}\frac{\partial \hat{\mathscr{F}}_1}{\partial \phi} \end{aligned}\right\} \tag{2.28}$$

where ε_2, which equals $\varepsilon_1^{-3/4}$, represents the ratio of u_F to u_B in the thermal boundary layer of the present region. The resulting governing equations are

$$\frac{\partial^3 \hat{\mathscr{F}}_1}{\partial \zeta^3} + \hat{\mathscr{H}}_1 \sin\phi = 0 \tag{2.29}$$

$$\frac{\partial^2 \hat{\mathscr{H}}_1}{\partial \zeta^2} + \frac{\partial \hat{f}}{\partial \phi}\frac{\partial \hat{\mathscr{H}}_1}{\partial \zeta} - \frac{\partial \hat{f}}{\partial \zeta}\frac{\partial \hat{\mathscr{H}}_1}{\partial \phi} - \frac{\partial \hat{\mathscr{F}}_1}{\partial \zeta}\frac{\partial \hat{h}}{\partial \phi} + \frac{\partial \hat{\mathscr{F}}_1}{\partial \phi}\frac{\partial \hat{h}}{\partial \zeta} = \frac{\alpha}{4}\zeta^2 \frac{\partial \hat{h}}{\partial \zeta} \tag{2.30}$$

$$\begin{aligned} \hat{\mathscr{F}}_1(0,\phi) = 0 = \frac{\partial \hat{\mathscr{F}}_1}{\partial \zeta}(0,\phi) = \hat{\mathscr{H}}_1(0,\phi) \\ = \frac{\partial^2 \hat{\mathscr{F}}_1}{\partial \zeta^2}(\infty,\phi) = \hat{\mathscr{H}}_1(\infty,\phi). \end{aligned} \tag{2.31}$$

Due to the form of the inhomogeneous forcing term on the r.h.s. of (2.30), a similarity solution for $\hat{\mathscr{F}}_1$ and $\hat{\mathscr{H}}_1$ is precluded. Hence, a Blasius-series solution is appropriate and, since $\hat{f}$ and $\hat{h}$ are most simply described in terms of η and ξ, the series will be taken in η and ξ rather than ζ and ϕ. That is,

$$\left.\begin{aligned} &\hat{\mathscr{F}}_1(\zeta,\phi) = \xi^{3/4}\mathscr{F}_1(\eta,\xi) = \xi^{3/4}\sum_{n=0}^{\infty} \xi^{3n/2}\mathscr{F}_{1n}(\eta) \\ &\hat{\mathscr{H}}_1(\zeta,\phi) = \mathscr{H}_1(\eta,\xi) \quad = \sum_{n=0}^{\infty} \xi^{3n/2}\mathscr{H}_{1n}(\eta). \end{aligned}\right\} \tag{2.32}$$

Substitution into (2.29)–(2.30) and collection of terms in like powers of ξ results in (with $b \equiv (3/4)^{3/4}$):

$O(\xi^0)$:

$$\left.\begin{aligned} \mathscr{F}_{10}''' + \mathscr{H}_{10} &= 0 \\ \mathscr{H}_{10}'' + \tfrac{3}{4} f \mathscr{H}_{10}' + \tfrac{3}{4}\mathscr{F}_{10} h' &= \frac{b}{4}\alpha\eta^2 h' \end{aligned}\right\} \tag{2.33}$$

$O(\xi^{3/2})$:

$$\left.\begin{aligned} \mathscr{F}_{11}''' + \mathscr{H}_{11} &= 0 \\ \mathscr{H}_{11}'' + \tfrac{3}{4} f \mathscr{H}_{11}' - \tfrac{3}{4} f' \mathscr{H}_{11} + \tfrac{9}{4}\mathscr{F}_{11} h' &= \frac{3\alpha}{80b}\eta^2 h' \end{aligned}\right\} \tag{2.34}$$

with the process continuing to all integral powers of $\xi^{3/2}$. For all $n \geqslant 0$, the associated boundary conditions are:

$$\mathscr{F}_{1n}(0) = 0 = \mathscr{F}'_{1n}(0) = \mathscr{H}_{1n}(0) = \mathscr{F}''_{1n}(\infty) = \mathscr{H}_{1n}(\infty). \tag{2.35}$$

Numerical integration gives:

$$\left.\begin{aligned} \mathscr{F}''_{10}(0) &= 0{\cdot}081096, \quad \mathscr{H}'_{10}(0) = 0{\cdot}029579, \\ \mathscr{F}'_{10}(\infty) &= 0{\cdot}133333 \\ \mathscr{F}''_{11}(0) &= 0{\cdot}0072809, \quad \mathscr{H}'_{11}(0) = 0{\cdot}0023300, \\ \mathscr{F}'_{11}(\infty) &= 0{\cdot}014230. \end{aligned}\right\} \tag{2.36}$$

Hence, in particular, the perturbation effect of the forced flow in this region is to decrease the heat transfer.

Due to the non-linear thermal-convection effect, it is clear that the interaction between $\hat{\mathscr{F}}_1$ and $\hat{\mathscr{H}}_1$ gives rise to smaller-order terms, of $O(\varepsilon_2^2)$, and that, in fact, there exists an infinite series in powers of ε_2. In particular, it is found that (see [13]):

$$\left.\begin{aligned} \mathscr{F}''_{20}(0) &= 0{\cdot}033405, \quad \mathscr{H}'_{20}(0) = 0{\cdot}0083467, \\ \mathscr{F}'_{20}(\infty) &= 0{\cdot}073348 \\ \mathscr{F}''_{21}(0) &= 0{\cdot}0036312, \quad \mathscr{H}'_{21}(0) = 0{\cdot}00045047, \\ \mathscr{F}'_{21}(\infty) &= 0{\cdot}0092663. \end{aligned}\right\} \tag{2.37}$$

(d) *The far-intermediate region*

It is apparent that the axially-invariant structure of the intermediate region cannot be sustained indefinitely since eventually the rise in the bulk temperature must become significant and interact with the thermal boundary layer. In particular, a global energy-rate balance based upon the intermediate-region structure gives

$$\rho\pi a^2 W_0 c_p \frac{\mathrm{d}T_b}{\mathrm{d}z} \sim 2\pi a k \frac{\Delta T}{\delta_B}$$

from which it follows that ΔT_b becomes of $O(\Delta T)$ where

$$\frac{z}{aR} = O\left(\frac{P^{3/4}}{G^{1/4}}\right). \tag{2.38}$$

That is, once z satisfies (2.38), the thermal boundary layer is effectively developing within a z-dependent external temperature field and, hence, must itself be z-dependent. Therefore, the theory in (b) is restricted to the region

$$O\left(\frac{P^{1/6}}{G^{1/2}}\right) < \frac{z}{aR} < O\left(\frac{P^{3/4}}{G^{1/4}}\right). \tag{2.39}$$

A means of analyzing the effect of the bulk-temperature rise upon the thermal boundary layer is by forming a perturbation expansion based upon the quantity

$$\varepsilon_3 \equiv \frac{z}{aR}\left(\frac{G^{1/4}}{P^{3/4}}\right). \tag{2.40}$$

In particular, the limiting governing equations and boundary conditions on u, v and T are the same as in (b) provided "T_0" is everywhere replaced by "T_b". Hence, appropriate expansions in this far-intermediate region are given by:

$$\left.\begin{aligned} \psi &= V_B \delta_B \xi^{3/4} \sum_{n=0}^{\infty} \varepsilon_3^n f_n(\eta) \\ (T - T_b) &= \Delta T \sum_{n=0}^{\infty} \varepsilon_3^n h_n(\eta) \end{aligned}\right\} \tag{2.41}$$

where f_0 and h_0 are the same as f and h of (b). Substitution of (2.41) into the limiting governing equations and collection of terms in like powers of ε_3 results in ($n \geqslant 0$):

$$f_n''' + h_n = 0; \quad h_n'' + \sum_{k=0}^{n} f_{n-k} h_k' = 0 \tag{2.42}$$

subject to the four homogeneous boundary conditions,

$$f_n(0) = 0 = f_n'(0) = f_n''(\infty) = h_n(\infty) \tag{2.43}$$

and a fifth condition, on $h_n(0)$, which is obtained immediately below.

From the definition of T_b, it follows that

$$T_b(z) - T_0 = \frac{1}{\rho\pi a^2 W_0 c_p} \int_0^z \int_0^{2\pi} \left\{ k \left(\frac{\partial T}{\partial r} \right)_{r=a} \right\} a \, \mathrm{d}\phi \, \mathrm{d}z.$$

Hence, evaluating this integral on the basis of (2.41) (i.e. neglecting the bulk-temperature rise of the near region—an assumption which will be corrected for, approximately, in Section 3), it follows that

$$T_b - T_0 = \Delta T \sum_{n=1}^{\infty} C_n \varepsilon_3^n \tag{2.44}$$

where

$$C_n = -\frac{2}{\pi} \frac{h'_{n-1}(0)}{n} \int_0^{\pi} \frac{\sin^{1/3}\phi}{\xi^{1/4}} \mathrm{d}\phi. \tag{2.45}$$

Therefore, since the isothermal wall condition requires that

$$T_W - T_b = \Delta T \sum_{n=0}^{\infty} \varepsilon_3^n h_n(0) \tag{2.46}$$

it follows from (2.44) and (2.46) that

$$h_0(0) = 1, \quad h_n(0) = -C_n \quad (n \geqslant 1). \tag{2.47}$$

Since C_n is known once h_{n-1} has been determined, it follows that the h_n can be obtained successively. In particular, numerical integration of (2.42) subject to (2.43) and (2.47) results in the following values for $n = 0$ through 5:

$$\left.\begin{aligned} f_n''(0) &= 1{\cdot}16604, \ -0{\cdot}76130, \ 0{\cdot}33136, \\ &\quad -0{\cdot}12019, \ 0{\cdot}03924, \ -0{\cdot}01195 \\ h_n'(0) &= -0{\cdot}50275, \ 0{\cdot}54706, \ -0{\cdot}35717, \\ &\quad 0{\cdot}18137, \ -0{\cdot}07894, \ 0{\cdot}03093 \end{aligned}\right\} \tag{2.48}$$

with the associated values of C_n for $n = 1$ through 6 given by:

$$C_n = 0{\cdot}87052,\ -0{\cdot}47363,\ 0{\cdot}20615,\ -0{\cdot}07851,\ 0{\cdot}02734,\ -0{\cdot}00892. \quad (2.49)$$

(e) *The far region*

Since the buoyant effect is proportional to the temperature variation within the fluid, it is clear that the natural convection must diminish as $(T_w - T_b)/\Delta T$ becomes small. Hence, the forced convection must eventually reappear as the dominant transport mechanism with the final asymptotic development of the temperature field corresponding to that of the Graetz problem.

That is, as $z/(aR)$ becomes of $O(P)$, $(T_w - T_b)/\Delta T$ approaches zero exponentially fast as $A_1 e^{-\alpha_1 z/(aRP)}$ where $\alpha_1 = 3{\cdot}657$ is the first eigenvalue from the Graetz problem and A_1 is a constant whose value would be extremely difficult to determine, being dependent upon the far-intermediate region and subsequent development. Qualitatively, however, since the natural convection effectively annihilates itself where $z/(aR) = O(P^{3/4}/G^{1/4})$, it follows that the forced convection should be significant in the region

$$O\left(\frac{P^{3/4}}{G^{1/4}}\right) < \frac{z}{aR} \leqslant O(P), \quad (2.50)$$

becoming the dominant (howbeit, weak) transport mechanism towards the latter part of this region. Since $(GP)^{1/4}$ appears as the ratio of the upper to lower bound in (2.50), it seems reasonable to expect that A_1 will be mainly a function of $(GP)^{1/4} - a$ monotonically decreasing function, at that (as is clear on a physical basis).

Since a detailed solution for this region would be extremely complicated, it is indeed fortunate that such a solution may be omitted without much loss since $(T_w - T_b)/\Delta T$ is uniformly small throughout this region. That is, as far as the heat transfer is concerned, main interest lies in determining where $(T_w - T_b)/\Delta T$ first becomes small, which corresponds identically with where the natural convection destroys itself, namely in the far-intermediate region.

3. DISCUSSION

Based upon the previous section it follows that if $G > O(P^{1/3})$ and the inlet velocity is uniform then the local (in ϕ and z) Nusselt number in the near region, (2.15), is given by

$$N = P^{1/3}\left(\frac{z}{aR}\right)^{-1/2}[0{\cdot}3387 + \varepsilon_1(0{\cdot}2177\cos\phi) + \varepsilon_1^2(-0{\cdot}0558 + 0{\cdot}2849\sin^2\phi) + O(\varepsilon_1^3)] \quad (3.1)$$

whereas, in the intermediate region, (2.39),

$$N = (GP)^{1/4}\frac{\sin^{1/3}\phi}{\xi^{1/4}}[0{\cdot}5027 + \Lambda_1 + \Lambda_2] \quad (3.2)$$

where Λ_1 is the near-intermediate-region contribution,

$$\Lambda_1 \equiv \left.\begin{aligned}&\varepsilon_2\{-0{\cdot}02958 - 0{\cdot}002330\,\xi^{3/2} + O(\xi^3)\} + \varepsilon_2^2 \\ &\times\{-0{\cdot}008347 - 0{\cdot}0004505\,\xi^{3/2} + O(\xi^3)\} + O(\varepsilon_2^3)\end{aligned}\right\} \quad (3.3)$$

and Λ_2 that of the far-intermediate:

$$\Lambda_2 \equiv -0{\cdot}5471\,\varepsilon_3 + 0{\cdot}3572\,\varepsilon_3^2 - 0{\cdot}1814\,\varepsilon_3^3 + 0{\cdot}07894\,\varepsilon_3^4 - 0{\cdot}0309\,\varepsilon_3^5 + O(\varepsilon_3^6). \quad (3.4)$$

These results are illustrated in Fig. 1 at $\phi = 0°$ and $G = 10^4$, $P = 10^2$ and $R = 400$. Curves 0, 1, and 2 are based upon the near-region theory, (3.1), with "0" denoting the purely forced-flow result; curve 0′ is the zeroth-order result of the intermediate-region theory; (3.2), with 1′ and 2′ corresponding to the retention of one and two terms in Λ_1. The final sloping down of the curve for large z/a is due to Λ_2. It is seen that the curves based upon (3.1) and (3.2) merge very well with each other, the solid curve being the composite result based upon graphical interpolation between the two. A local minimum in N is apparent.

Averaged over ϕ, the above reduce to:

$$\bar{N} = P^{1/3}\left(\frac{z}{aR}\right)^{-1/2}[0{\cdot}3387 + 0{\cdot}0867\,\varepsilon_1^2 + O(\varepsilon_1^3)] \quad (3.5)$$

and

$$\bar{N} = (GP)^{1/4}[0{\cdot}4353 - 0{\cdot}0287\,\varepsilon_2 - 0{\cdot}0078\,\varepsilon_2^2 + O(\varepsilon_2^3) + 0{\cdot}8657\,\Lambda_2]. \quad (3.6)$$

These results are illustrated in Fig. 2 where $\bar{N}$ vs z/a has been plotted for $P = 10^2$, $R = 400$ and $G = 10^3$, 10^4, 10^5. Curve A is based upon the first term in (3.5) and curves B upon the first in (3.6); also shown is the $O(\varepsilon_1^2)$ contribution from the near region and the contribution, to $O(\varepsilon_2^2)$, of the near-intermediate; curves (ii) and (iii) are based upon the retention of two and three terms in Λ_2, respectively. As above, the curves are seen to merge well, the solid curve being the composite result based upon graphical interpolation.

Since main interest lies in determining the bulk-temperature rise of the fluid, it would be desirable to integrate the above result over z in order to obtain the average Nusselt number for the entire pipe, $\bar{N}$, which is related to ΔT_b by:

$$\bar{N} = \left(\frac{aRP}{2L}\right)\frac{\Delta T_b}{\Delta T}. \quad (3.7)$$

However, such a procedure would be complicated by the necessity of obtaining an analytic expression for $\bar{N}$ in the "interpolated" region in which neither (3.5) nor (3.6) is applicable. Rather, the procedure below will be to compare available data directly with the theory of the far-intermediate region, since it is here that $\Delta T_b/\Delta T$ first becomes appreciable. Higher-order corrections will then be made upon the far-intermediate theory.

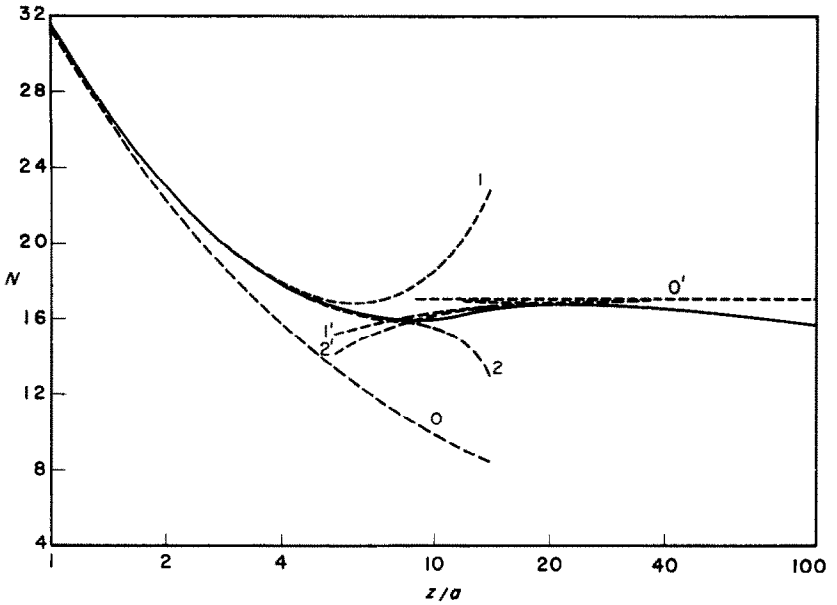

FIG. 1. Variation of local Nusselt number with z/a at $\phi = 0$ and $G = 10^4$, $P = 10^2$, $R = 400$.

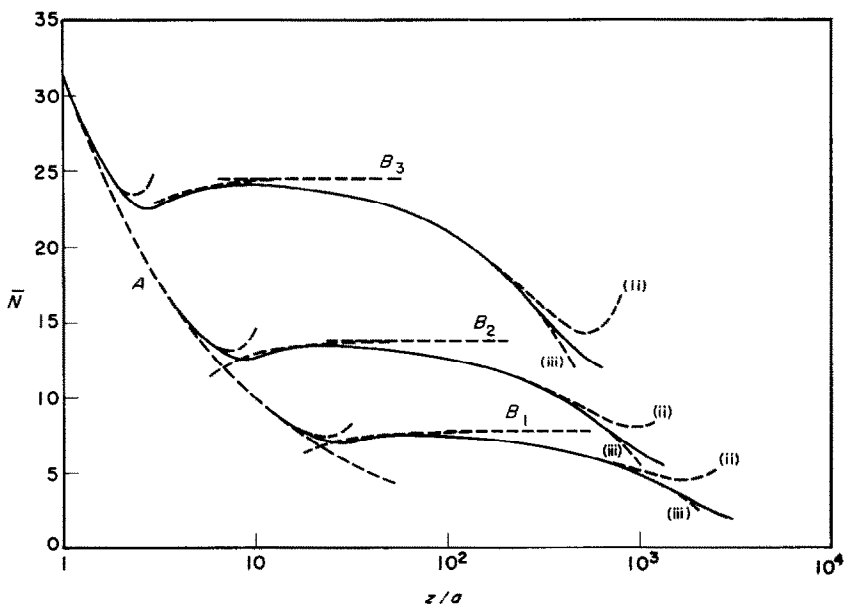

FIG. 2. Variation of ϕ-averaged Nusselt number with z/a for $P = 10^2$, $R = 400$ and $G = 10^3, 10^4, 10^5$. ("B_3" corresponds to $G = 10^5$.)

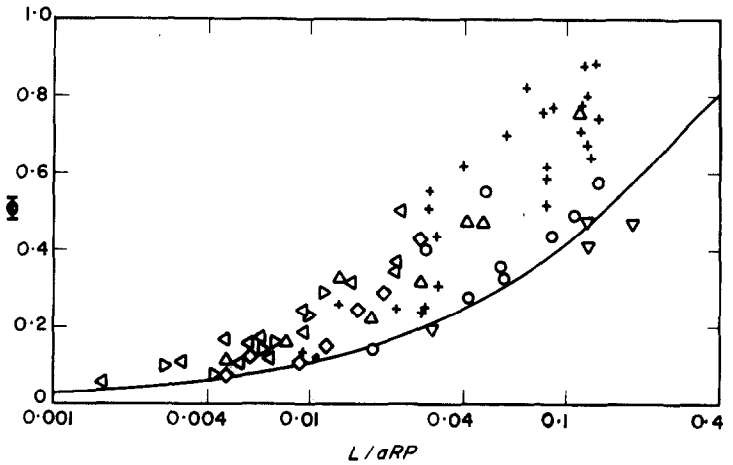

FIG. 3. Φ vs $L/(aRP)$. +: water (Oliver, D&A, B&T); △: ethyl alcohol (Oliver, D&A); ○: 80:20 glycerol–water (Oliver, D&A); ▽: glycerol (Oliver); ◁: transformer oil (K&O); ▷: core oil (K&O); ◇: cylinder oil (K&O). Curve corresponds to Graetz solution.

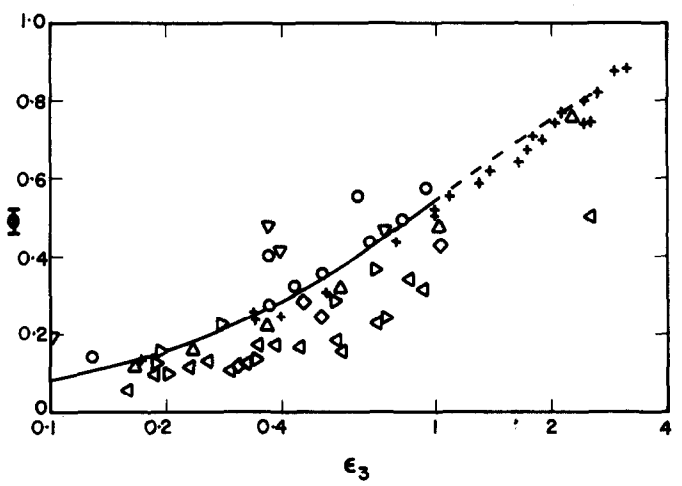

FIG. 4. Φ vs ε_3 (evaluated at $z = L$). Symbols have same meaning as in Fig. 3. Solid curve based upon first six terms of (2.44).

The only pertinent experimental investigations appear to have been those of Kern and Othmer [9], Oliver [10], Brown and Thomas [11] and Depew and August [12]. For reference purposes, the operating ranges of these experiments are indicated in Table 1. Every fourth data point of these investigations is shown in Fig. 3 in terms of

$$\Phi = \left(\frac{\mu_w}{\mu_a}\right)^{0.14} \left(\frac{\Delta T_b}{\Delta T}\right)_{\text{exp.}}$$

vs $L/(aRP)$. [A standard procedure has been employed in Figs. 3–4 whereby all fluid properties are evaluated at the average bulk temperature, T_a, and the measured $\Delta T_b/\Delta T$ is multiplied by the above viscosity-ratio factor.] The indicated curve in Fig. 3 corresponds to the Graetz solution. Clearly, with the exception of the glycerol and some of the 80:20 glycerol–water results, the data is systematically well above the forced-flow theory, suggesting the presence of an additional transport mechanism.

On the basis of the present theory, Φ has been plotted vs ε_3 (with $z = L$) in Fig. 4, wherein the solid curve is based upon the first six terms in (2.44). It is seen that all the water data (based upon three separate investigations) correlate very well with ε_3 and are in good agreement with the solid curve. On the basis of the

Table 1. Operating ranges of pertinent experimental investigations. Properties evaluated at T_a. (*R exceeded 10^3 in only two runs, neither of which is anomolous)

Fluid	Investigator(s)	L/a	R	P	G	$(GP)^{1/4}$	W_0(cm/s)	a(cm)	ΔT(°C)	$(\mu_w/\mu_a)^{0.14}$
water	Oliver	144	42,760	5·5, 8·8	2×10^3, 2×10^4	12, 19	0·7, 12	0·64	−10, 21	0·95, 1·03
	Brown and Thomas	72,216	118,810	3·6, 7·4	5×10^3, 9×10^5	13, 44	0·8, 9·0	0·64, 1·27	−33, −6	1·02, 1·11
	Depew and August	56·8	58,820	5·7, 8·0	1×10^4, 8×10^4	18, 26	0·7, 8·8	1·00	−22, −10	1·02, 1·06
ethyl–alcohol	Oliver	144	54,740	14, 18	9×10^3, 3×10^4	20, 25	1·1, 12	0·64	−12, 21	0·96, 1·03
	Depew and August	56·8	43,900	14, 17	4×10^4, 1×10^5	29, 36	0·6, 12	1·00	−21, −11	1·02, 1·05
80:20 glycerol–water	Oliver	144	1·8, 19	340, 600	4, 40	7, 10	1·4, 12	0·64	−12, 21	0·88, 1·10
	Depew and August	56·8	2·5, 10	330, 390	70, 100	13, 14	0·9, 3·5	1·00	−21, −20	1·14, 1·18
glycerol	Oliver	144	0·06, 0·30	$9{\cdot}5 \times 10^3$, $2{\cdot}1 \times 10^4$	4×10^{-3}, 3×10^{-2}	3, 4	1·2, 7·0	0·64	−13, 19	0·81, 1·11
transformer oil	Kern and Othmer	97,386	100, 1600*	35, 130	9×10^3, 5×10^6	32, 120	0·8, 71	0·79, 3·14	124, 220	0·65, 0·84
core oil	Kern and Othmer	97,386	35,200	170, 860	200, 3×10^5	21, 86	1·1, 86	0·79, 3·14	152, 215	0·58, 0·78
cylinder oil	Kern and Othmer	97,386	9, 91	450, 1700	50, 1×10^4	17, 56	1·8, 92	0·79, 3·14	148, 199	0·58, 0·74

trend in this water data, the theoretical curve has been extrapolated (dashed) and can be represented by

$$\Phi = 0{\cdot}543 + 0{\cdot}315(\varepsilon_3 - 1) - 0{\cdot}132(\varepsilon_3 - 1)^2 + 0{\cdot}028(\varepsilon_3 - 1)^3. \quad (3.8)$$

for $1 \leqslant \varepsilon_3 \leqslant 2{\cdot}5$. The ethyl–alcohol data are also seen to correlate very well with ε_3 although they are only in fair agreement with the theory, being systematically below the curve by about 15 per cent.

Concerning the 80:20 glycerol–water data, it is observed that many of the points are in close agreement with the theory but that some are systematically above the curve by 40–50 per cent. All of the latter points are from [12] and can be discredited on the basis of internal inconsistency. In particular, all eleven glycerol–water runs in [12] were obtained with essentially the same inlet bulk temperature and wall temperature, the only independent variable being the mass flow rate ($\dot{m}$). The latter was first increased from run 1 to 2, then decreased from run 2 to 3 and then monotonically increased from run 3 through 11. Although runs 1–3 are in fair agreement (10–20 per cent) with the theory, the remaining runs are not. The inconsistency amongst these data points is seen, e.g. by comparing run 1 (2) with run 7 (10). Although $\dot{m}$ in the latter run is larger by 6 per cent (3 per cent), the value of ΔT_b is also larger, and by 30 per cent (35 per cent).

Most of the glycerol data in Fig. 4 is seen to differ markedly from the theoretical curve. This is to be expected since these runs were actually forced-flow dominated, as evidenced in Fig. 3. In fact, Oliver's objective in using glycerol was merely to check his apparatus by making comparison with the known forced-flow theory.

The data of Kern and Othmer are seen to be typically well below the theoretical curve in Fig. 4. In examining their data, it is to be noted that three different sized pipes ($a = 3{\cdot}14$ cm, $1{\cdot}53$ cm and $0{\cdot}79$ cm) were used in each of the three oils and that a systematic trend towards the theory is evidenced with decreasing radius. (In fact, most of the core-oil and cylinder-oil data in the smallest pipe are well within 10 per cent of the theory.) This systematic trend, which is apparently due to a G-dependent effect, could perhaps be attributable to the large values ($\approx 10^8$) of GP in the larger pipes and the resulting possibility of a breakdown in the thermal boundary layer arising from a thermally unstable situation at $\phi = 0$. In any event, it is clear that this systematic dependence upon pipe radius is not explainable in terms of the present theory.

A more refined comparison with the data can be obtained by making corrections upon the intermediate-region theory in order to account for such higher-order effects as the near-region contribution to $\Delta T_b/\Delta T$ and that of finite P and $(GP)^{1/4}$. The former effect can be represented in terms of an effective increase in pipe length with the resulting increase in ε_3 being given by (see [13]):

$$\Delta\varepsilon_3 \simeq 0{\cdot}61/(G^{1/4}P^{7/12}) \quad (3.9)$$

if the inlet flow is uniform and $G > O(P^{1/3})$ or by

$$\Delta\varepsilon_3 \simeq 3{\cdot}8/(GP)^{1/2} \quad (3.10)$$

if the inlet flow is fully developed or the inlet flow is uniform but $O(P^{-1}) < G < O(P^{1/3})$. Regarding the effects of a finite P and $(GP)^{1/4}$ upon the intermediate-region structure, it is noted that if $G > O(P)$ then the thermal boundary layer becomes imbedded within a velocity boundary layer, of order $a(P/G)^{1/4}$ in thickness, and the interaction between the two layers reduces the ϕ-averaged heat flux of (2.25) by the multiplicative factor (see [13]):

$$(1 - 0{\cdot}244\,P^{-1/2} + 0{\cdot}10\,P^{-1}). \quad (3.11)$$

If $G < O(P)$, then the thermal boundary layer becomes imbedded within a viscous core which interacts with the boundary layer and reduces (2.25) by the factor (see [13]):

$$(1 - 1{\cdot}10/(GP)^{1/2}). \quad (3.12)$$

For simplicity, it will be assumed that these correction factors multiply not only the first, but all, of the terms in (2.44).

A summary of the resulting correlation between data and theory (based upon first six terms in (2.44) for $\varepsilon_3 < 1$ and upon (3.8) for $1 \leqslant \varepsilon_3 \leqslant 2{\cdot}5$) is given in Table 2. For comparison, it is noted that the most recent empirical correlation, in [12], gives agreement with the data in Table 2 (glycerol omitted) to within ± 40 per cent. However, in so doing, much of the water and ethyl–alcohol data of Oliver lie 20–40 per cent below the empirical curve while much of the data of Brown and Thomas lie 20–40 per cent above. In light of the present investigation, it appears that the previous empirical correlations have suffered from seeking order amongst some rather irreconcilable data.

Lastly, according to the present theory, it is noted that the temperature field outside of the thermal boundary layer is essentially only z-dependent. Although this can be shown to be a self-consistent structure (see [13]), the results obtained in investigations of analogous problems [3, 6, 7, 15] suggest that thermal stratification may exist outside of the thermal boundary layer in the present problem also. If so, the analysis would be much more difficult although the heat-transfer rates would probably be not much different (e.g. the approximate solution in [6] for the stratified case of that problem results in $\bar{N} = 0{\cdot}471\,(GP)^{1/4}$ as compared with $0{\cdot}435\,(GP)^{1/4}$ for the non-stratified case). From a fundamental point of view,

Table 2. Comparison of theory and data. Bracketed values in last two columns are based upon higher-order corrections (the first upon near-region correction, the second upon both)

Fluid	Investigators	No. of data pts.	avg dev (%)	RMS dev wrt avg (%)
water	Oliver heated	10	−10 (−11) (−3)	3 (3) (4)
	Oliver cooled	7	−5 (−7) (0)	2 (4) (4)
	Depew and August	15	−6 (−8) (0)	6 (7) (7)
	Brown and Thomas	57	−3 (−4) (5)	3 (3) (3)
ethyl–alcohol	Oliver heated	11	−16 (−16) (−12)	3 (3) (3)
	Oliver cooled	7	−9 (−10) (−5)	8 (9) (9)
	Depew and August	12	−11 (−12) (−7)	10 (10) (10)
80:20 glycerol–water	Oliver heated	18	11 (−10) (5)	12 (6) (5)
	Oliver cooled	7	19 (−3) (14)	15 (7) (7)
	Depew and August	11	42 (35) (47)	13 (12) (12)
glycerol	Oliver heated	15	59 (−52) (−31)	23 (31) (27)
	Oliver cooled	4	128 (−43) (−10)	14 (7) (8)
transformer oil	Kern and Othmer $a = 3{\cdot}14$ cm	20	−47 (−47) (−46)	10 (10) (10)
	Kern and Othmer $a = 1{\cdot}53$ cm	15	−39 (−39) (−37)	11 (11) (11)
	Kern and Othmer $a = 0{\cdot}79$ cm	16	−32 (−32) (−31)	3 (3) (4)
core oil	Kern and Othmer $a = 3{\cdot}14$ cm	23	−43 (−43) (−42)	10 (10) (10)
	Kern and Othmer $a = 1{\cdot}53$ cm	18	−27 (−28) (−27)	11 (11) (11)
	Kern and Othmer $a = 0{\cdot}79$ cm	20	−3 (−6) (−5)	7 (7) (7)
cylinder oil	Kern and Othmer $a = 3{\cdot}14$ cm	11	−45 (−45) (−45)	7 (7) (7)
	Kern and Othmer $a = 1{\cdot}53$ cm	11	−32 (−32) (−32)	7 (7) (7)
	Kern and Othmer $a = 0{\cdot}79$ cm	11	−2 (−11) (−10)	12 (10) (10)

then, it would be highly desirable to make a thorough and detailed experimental investigation of the present problem in order to ascertain the presence or absence of stratification and, further, to determine in what range of $(GP)^{1/4}$ the laminar flow becomes unstable.

REFERENCES

1. B. R. Morton, Laminar convection in uniformly heated horizontal pipes at low Rayleigh numbers, *Q. Jl Mech. Appl. Math.* **12**, 410–420 (1959).
2. E. del-Casal and W. N. Gill, A note on natural convection effects in fully-developed horizontal tube flow, *A.I.Ch.E. Jl* **8**, 570–574 (1962).
3. R. D. Mikesell, The effect of heat transfer on the flow in a horizontal pipe, Ph.D. Thesis, Univ. Illinois (1963).
4. G. N. Faris and R. Viskanta, An analysis of laminar combined forced and free convection heat transfer in a horizontal tube, *Int. J. Heat Mass Transfer* **12**, 1295–1309 (1969).
5. Y. Mori and K. Futagami, Forced convective heat transfer in uniformly heated horizontal tubes, *Int. J. Heat Mass Transfer* **10**, 1801–1813 (1967).
6. D. P. Siegwarth, R. D. Mikesell, T. C. Readal and T. J. Hanratty, Effect of secondary flow on the temperature field and primary flow in a heated horizontal tube, *Int. J. Heat Mass Transfer* **12**, 1535–1552 (1969).
7. D. P. Siegwarth and T. J. Hanratty, Computational and experimental study of the effect of secondary flow on the temperature field and primary flow in a heated horizontal tube, *Int. J. Heat Mass Transfer* **13**, 27–42 (1970).
8. P. H. Newell and A. E. Bergles, Analysis of combined free and forced convection for fully developed laminar flow in horizontal tubes, *J. Heat Transfer* **92**, 83–93 (1970).
9. D. Q. Kern and D. F. Othmer, Effect of free convection on viscous heat transfer in horizontal tubes, *Trans. Am. Inst. Chem. Engrs* **39**, 517–555 (1943).
10. D. R. Oliver, The effect of natural convection on viscous-flow heat transfer in horizontal tubes, *Chem. Engng Sci.* **17**, 335–350 (1962).
11. A. R. Brown and M. A. Thomas, Combined free and forced convection heat transfer for laminar flow in horizontal tubes, *J. Mech. Engng Sci.* **7**, 440–448 (1965).
12. C. A. Depew and S. E. August, Heat transfer due to combined free and forced convection in a horizontal and isothermal tube, *J. Heat Transfer* **93**, 380–384 (1971).
13. S. K. Sreenivasan, Ph. D. Thesis, Clarkson College of Technology (1974).
14. A. Acrivos, A theoretical analysis of laminar natural convection heat transfer to non-Newtonian fluids, *A.I.Ch.E. Jl* **6**, 584–590 (1960).
15. A. E. Gill, The boundary-layer regime for convection in a rectangular cavity, *J. Fluid Mech.* **26**, 515–536 (1966).

CONVECTION MIXTE DANS UN TUBE HORIZONTAL ET ISOTHERME

Résumé—Une étude théorique concerne l'écoulement laminaire d'un fluide, à grand nombre de Prandtl, dans un tube horizontal et chauffé de façon isotherme. On obtient une solution analytique qui montre, en première approximation, que l'élévation de la température de mélange est seulement une fonction de $(L/aR)(G/P^3)^{1/4}$. La théorie s'accorde bien avec les résultats expérimentaux connus et constitue une amélioration marquée des expressions empiriques actuelles.

GEMISCHTE KONVEKTION IN EINEM WAAGERECHTEN, ISOTHERM BEHEIZTEN ROHR

Zusammenfassung—Die laminare Strömung eines Fluids mit hoher Prandtl-Zahl in einem waagerechten, isotherm beheizten Rohr wird untersucht. Die erhaltene ausführliche analytische Lösung zeigt, daß mit guter Näherung der partielle Anstieg der Kerntemperatur allein eine Funktion von $(L/aR)(G/P^3)^{1/4}$ ist. Die Theorie zeigt sehr gute Übereinstimmung mit verfügbaren experimentellen Ergebnissen und stellt eine bemerkenswerte Verbesserung im Vergleich zu vorhandenen empirischen Beziehungen dar.

СМЕШАННАЯ КОНВЕКЦИЯ В ИЗОТЕРМИЧЕСКИ НАГРЕВАЕМОЙ ГОРИЗОНТАЛЬНОЙ ТРУБЕ

Аннотация — Теоретически исследуется ламинарное течение жидкости в изотермически нагреваемой горизонтальной трубе при больших числах Прандтля. Полученное подробное аналитическое решение показывает в основном приближении, что увеличение относительной температуры жидкости есть только функция $(L/aR)(G/P^3)^{1/4}$. Найдено, что теоретические расчеты хорошо согласуются с имеющимися экспериментальными результатами и вносят значительный вклад в существующие эмпирические корреляции.